ELSEVIER

Mechanics of Materials 32 (2000) 85–97

MECHANICS OF MATERIALS

www.elsevier.com/locate/mechmat

An approximate method for residual stress calculation in functionally graded materials

T.L. Becker Jr. [b], R.M. Cannon [a], R.O. Ritchie [a,*]

[a] *Department of Materials Science and Mineral Engineering, and Materials Sciences Division, Lawrence Berkeley National Laboratory, University of California, Berkeley, CA 94720-1760, USA*

[b] *Department of Mechanical Engineering, and Materials Sciences Division, Lawrence Berkeley National Laboratory, University of California, Berkeley, CA 94720-1760, USA*

Received 3 June 1999

Abstract

Thermal residual stresses in functionally graded materials (FGMs) arise primarily from nonlinear spatial variations in the thermal expansion coefficient, but can be significantly adjusted by variations in modulus. Thermoelastic analysis of FGMs is complicated by such modulus gradients. A class of problems for which thermal stress solutions for materials with constant modulus can be used as a basis for approximations for FGMs is discussed. The size of the error in this approximation due to gradients in elastic modulus is investigated. Analytical and finite element solutions for the thermal stresses in various FGM geometries are compared to results from this approximate method. In a geometry of practical interest, a right cylinder graded along the z-axis, the error for a Ni–Al_2O_3 FGM was found to be within 15% for all gradients considered. The form of the approximation makes it easier to identify desirable types of spatial nonlinearity in expansion coefficient and variations in modulus; this would allow the manipulation of the location of compressive stresses.

Keywords: FGM; Residual stress

1. Introduction

Functionally graded materials (FGMs), like other composites, are designed to achieve levels of performance superior to that of homogeneous materials by combining desirable properties of the constituent phases. However, unlike other composites, the composition of a FGM varies over length scales that are significant in comparison to the overall dimensions of the body. The shape of this material gradient is an important factor in determining the properties of an FGM structure. FGMs are often made of graded mixtures of two phases. As a result, at small length scales the shape of the gradient is of little importance, and the mechanics are dominated by the size, shape and interface conditions of a particle of one material embedded in the matrix of another. Mechanics analysis of an FGM usually emphasizes the larger-scaled phenomenon and employs only the "effective" properties of the composite at any given location. It is through the variation of these effective material properties (such as thermal

* Corresponding author. Tel.: +1-510-486-5798; fax: +1-510-486-4995.

E-mail address: roritchie@lbl.gov (R.O. Ritchie).

0167-6636/00/$ - see front matter
PII: S0167-6636(99)00042-3

expansion coefficient and modulus) that the nature of the spatial variations of the composition affects the mechanical behavior of the FGM.

As in many joining and composites problems, the effect of residual stress, arising either from processing or from in-service temperature variations, takes on an important role. The determination of the optimal thermal stress state needs to incorporate the thermal and mechanical properties of the constituents as well as their variation. The optimization of such stresses is a critical design goal and a driving force in FGM research. Indeed, several studies have focused on the theoretical and experimental (Delfosse et al., 1992) assessment of these stresses in FGMs. Simple analyses yield results for which residual stress can be eliminated (e.g., Giannakopoulos et al., 1995); however, this may not provide the optimum mechanical performance. The generation of surface compressive residual stress can result in superior strengths and fracture resistance compared to the stress-free configuration for both ductile and brittle materials (e.g., shot-peened aircraft components and tempered glass, respectively).

The effect of composition shape on residual thermal stresses has been studied for both the elastic and elastic-plastic conditions (Rabin et al., 1998; Giannakopoulos et al., 1995; Grujicic and Zhao, 1998). However, the complicating effect of modulus variation with position severely limits the scope of problems that can be solved analytically. A majority of this analytical work has been for FGM films or other simple structures, for which geometric assumptions allow for much simplified 1-D linear elastic calculations (Lutz and Zimmerman, 1996; Ravichandran, 1995; Obata and Noda, 1994; Tanaka et al., 1996; Tanigawa et al., 1996; Markworth and Saunders, 1995). For a more general 2-D or 3-D problem, numerical methods such as finite element analysis (FEA) are required. These are, by comparison, costly, as a full analysis for each material pairing, geometry and gradient must be performed.

In the present study, a method for estimating the influence of elastic gradients on the residual stress state of an FGM is considered. Analytical thermal stress solutions as well as finite element calculations are used for a variety of problems with varying modulus. Model material systems, $Mo–SiO_2$ and $Ni–Al_2O_3$, were used for numerical examples. The approximate method was found to be very accurate for a number of important problems. The use of this methodology allows for the application of thermal stress solutions for homogeneous materials to FGMs.

2. Problem formulation

The full description of the thermal stress problem in an FGM must include the variation in modulus. However, most standard thermoelastic analyses pertain to materials with constant E. These equations are recapitulated to provide groundwork for the discussion of the FGM problem.

2.1. Residual thermal stresses in elastically homogeneous bodies

The residual thermal stress state of an elastic body subject to temperature change ΔT is considered. This ΔT is assumed to vary smoothly with position in one arbitrary direction (with Cartesian coordinate x) and will be described by a polynomial function of position, $\Delta T(x) = \sum_{i=0}^{m} \delta_i x^i$. For a homogeneous thermoelastic body with free boundaries and constant coefficient of thermal expansion (CTE) α, Young's modulus E and Poisson's ratio v, stresses can be computed from the spatial derivatives of the Goodier potential (Boley and Winer, 1985). This potential is obtained from a weighted integration of the temperature field over the body. The stresses are therefore linearly related to each of the coefficients of the temperature field, δ_i, or equivalently, to $\alpha\delta_i$.

A smoothly varying composition in an FGM will result in smoothly varying effective thermomechanical properties, and the Goodier potential argument can be used to analyze the residual stresses arising from CTE gradients in elastically homogeneous materials. This is true because temperature change and CTE only appear as the product $\alpha\Delta T$ in the uncoupled thermoelastic problem and therefore the Goodier framework for

$\Delta T(x) * \alpha$ solves the identical problem [1] as for $\alpha(x) * \Delta T$. The problem of variable $\alpha(x)$ and constant ΔT is representative of the behavior of an FGM after processing at high temperature, e.g. sintering or CVD.

For FGMs, it is natural to formulate the problem in terms of the gradient in the composition, rather than directly in terms of $\alpha(x)$. Assuming that the volume fraction, v, of material #2 in a matrix of material #1 varies as a polynomial function in one dimension:

$$v(x) = v_0 + v_1 x^1 + v_2 x^2 + \cdots + v_n x^n = \sum_{i=0}^{n} v_i x^i \quad (1)$$

then with the coefficient of thermal expansion assumed to be a linear function of composition

$$\alpha = \alpha_1 + (\alpha_2 - \alpha_1)v = \alpha_1 + \Delta\alpha v \quad (2)$$

it follows that

$$\alpha(x) = \alpha_1 + v_0 \Delta\alpha + \sum_{i=1}^{n} \Delta\alpha v_i x^i. \quad (3)$$

For a material with constant modulus E_0, Eq. (3) combined with the implications of the Goodier potential arguments yields

$$\sigma_{jk} = \Delta\alpha \Delta T E_0 \sum_{i=1}^{n} v_i S^i_{jk} + (\alpha_1 + \Delta\alpha v_0)\Delta T E_0 S^0_{jk}, \quad (4)$$

where $S^i_{jk} = \sigma_{jk}/\Delta\alpha\Delta T E_0$ is the nondimensional *stress function* for the jk component of stress associated with degree i of the gradient polynomial. Practically, these stress functions can be obtained via the Goodier potential, or any other analytical, numerical or experimental method.

If variation of $\alpha\Delta T$ is linear in each of the Cartesian coordinates, then the body remains stress-free (Boley and Winer, 1985) and $S^0_{jk} = S^1_{jk} = 0$. Therefore,

$$\sigma_{jk} = \Delta\alpha \Delta T E_0 \sum_{i=2}^{n} v_i S^i_{jk}. \quad (5)$$

[1] This, of course, does not guarantee that there can exist such a steady-state temperature field, but rather if one existed, its stress state would be the same as that of the FGM under consideration.

This equation yields information on how the materials properties and the gradient shape affect the residual stress state of the FGM with constant modulus. Namely, the residual stresses are linear in the difference in thermal expansion, total temperature change, elastic modulus, and in each coefficient of a polynomial gradient shape, v_i.

2.2. Approximate solution for FGMs

Exact analytical solutions to problems with $E(x)$ are rare. To explore the possibility of constructing an approximate FGM solution from that of a homogenous body, the solution to the FGM problem is decomposed into two separate displacements,

$$\boldsymbol{u} = \boldsymbol{u}^0 + \boldsymbol{u}' \quad (6)$$

(see Fig. 1). The first displacement field, $\boldsymbol{u}^0$ represents the solution to the residual stress problem with $\alpha\Delta T(x)$ and a constant $E = E_0$ (Fig. 1(a)). The stresses that arise, $\boldsymbol{\sigma}^0$, are the same as in Eq. (5).

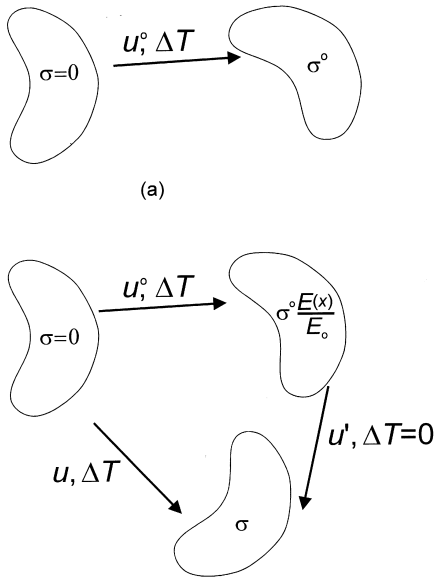

Fig. 1. (a) Motion of a homogeneous body with $E = E_0$ under thermal loading, $\alpha\Delta T(x)$, resulting in displacements $\boldsymbol{u}^0$ and stresses $\boldsymbol{\sigma}^0$. (b) Motion of an inhomogeneous body with $E = E(x)$. The displacements, $\boldsymbol{u}$, are decomposed into the homogeneous solution displacements, $\boldsymbol{u}^0$, and the displacements due to the modulus gradient, $\boldsymbol{u}'$.

Applying the linear strain–displacement equations, it follows that $\boldsymbol{\varepsilon} = \boldsymbol{\varepsilon}^0 + \boldsymbol{\varepsilon}'$. These strains can be substituted in the stress–strain relation (in indicial notation)

$$\sigma_{ij} = 2\varepsilon_{ij}\mu(x) + \lambda(x)\varepsilon_{kk}\delta_{ij} - (3\lambda(x) + 2\mu(x))\,\Delta T\alpha(x)\delta_{ij}, \tag{7}$$

$$\mu = \frac{E}{2(1+\nu)}, \quad \lambda = \frac{\nu E}{(1-2\nu)(1+\nu)}. \tag{8}$$

Identifying the stresses for the E_0 case and those associated with the displacements $\boldsymbol{u}'$:

$$\sigma^0_{ij} = 2\varepsilon^0_{ij}\mu_0 + \lambda_0\varepsilon^0_{kk}\delta_{ij} - (3\lambda_0 + 2\mu_0)\,\Delta T\alpha(x)\delta_{ij}, \tag{9}$$

$$\sigma'_{ij} = 2\varepsilon'_{ij}\mu(x) + \lambda(x)\varepsilon'_{kk}\delta_{ij}, \tag{10}$$

yields

$$\sigma_{ij} = \sigma^0_{ij}\frac{E(z)}{E_0} + \sigma'_{ij}. \tag{11}$$

For cases in which the stresses caused by the gradient are small,

$$\sigma_{ij} \approx \sigma^0_{ij}\frac{E(x)}{E_0}. \tag{12}$$

Formally, the analysis in Section 2.1 is only applicable to materials with homogeneous elastic constants. However, it is clear that Eq. (12) can be attained by substituting $E(x)$ for E_0 in Eq. (5), $\sigma_{jk} \approx \Delta\alpha\,\Delta T E(x)\sum_{i=2}^{n} v_i S^i_{jk}$.

Comparing Eqs. (11) and (12), it is clear that σ'_{ij} represents the error in the approximation, arising from modulus gradient-induced displacements, u'_i. This approximate method will be most successful in cases where the gradient in modulus affects the displacements the least. It is now possible to investigate the nature of this error. Enforcing the balance of linear momentum by taking "$\nabla\cdot$" on both sides of Eq. (11) and noting that $\nabla\cdot\boldsymbol{\sigma} = \nabla\cdot\boldsymbol{\sigma}^0 = \mathbf{0}$ leads to

$$\nabla\boldsymbol{\sigma}' + \frac{\nabla E(x)}{E_0}\cdot\boldsymbol{\sigma}^0 = 0. \tag{13}$$

These are the equilibrium equations for a material subjected to a body force. Now the problem of determining the error $\boldsymbol{\sigma}'$ is re-cast to that of the linear elastic problem of an inhomogeneous body ($E = E(x)$) with a traction-free surface, subjected not to a temperature change, but only to the body force $\boldsymbol{b} = (\nabla E(x)/E_0)\boldsymbol{\sigma}^0$. This, however, is still not a trivial problem and can only be used to identify the trends in the error.

Due to the linearity of this body force problem, it follows that the magnitude of the error stress will scale with $\boldsymbol{b}$, $\boldsymbol{\sigma}' \propto (\nabla E(x)/E_0)\boldsymbol{\sigma}^0$. More specifically, the error in the approximation enumerated in Eq. (12) scales linearly with: (1) the gradient of $E(x)$, and (2) with the magnitude of the stress in the homogeneous ($E = E_0$) solution. The first of these conclusions meets our expectations that at an interface between two materials with $E_1 \neq E_2$, the stresses are known to be singular, which here corresponds to the fact that ∇E is not defined.

In lieu of the solution to this body force problem, a number of FMG thermal stress problems are considered as examples of the application of the approximate method. In addition to a series of analytical solutions, finite element calculations have been performed for a FGM cylinder in order to explore a range of material combinations and gradient shapes and to determine the accuracy of the approximation.

3. Numerical procedures

In analyzing the thermal stresses of FGM's, we consider using the full finite element solution taking into account both CTE and modulus variation. The geometry chosen for FEA was a "short" cylinder (length to radius ratio, $L/R_0 = 5$), with the compositional gradient lying along the z-direction. The material composition is taken to be constant in both the radial and circumferential directions. However, this is a geometry for which symmetry places no useful (nontrivial) restrictions on the residual stress state (Hoger, 1986) and is not amenable to approximate methods that rely on Saint-Venant arguments (e.g., Nikishin, 1966). Two different material sets were considered, namely molybdenum–silica and nickel–alumina. The Mo–SiO_2 system is used in an arc-lighting application and the Ni–Al_2O_3 is a common model system for numerical studies, with application to

Table 1
Physical constants for the materials under study

	Molybdenum	SiO_2	Nickel	Al_2O_3
α (ave) (10^{-6} m/m)	5.72	0.5	16.43	8.8
E (GPa)	320	72	207	380
v	0.30 ($\approx$0.25)	0.20 ($\approx$0.25)	0.33 ($\approx$0.25)	0.23 ($\approx$0.25)

thermal barrier coatings. These represent two contrasting types of systems, with the higher coefficient of thermal expansion material having higher modulus in the first, and lower in the second. The room temperature moduli were used; however, the CTE that was used was the average between 25°C and 1000°C. The values of the constants are given in Table 1 (Touloukian, 1975; Touloukian, 1977).

The residual stresses were calculated via the finite element method, using the computer program FEAP (Zienkiewicz and Taylor, 1987). The problem was analyzed in axisymmetric mode using a mesh of 400–1100 nine-node quadrilateral elements. A special finite element was formulated such that Young's modulus and CTE varied in the z-direction *within* each element. In the formation of the stiffness matrix and the thermal loading vector, E and α were calculated at each Gauss point based on the value of the z-coordinate, thereby allowing quadratic variations within a single element. The CTE was assumed to be a linear function of composition (Eq. (2)). E was varied as a function of composition as prescribed by the Self Consistent Method (SCM) (Hill, 1965), which has been determined to be the micromechanical theory with the characteristics most desirable for analysis of FGMs [2] (Zuiker, 1995).

The difficulty of implementing the SCM is that it does not, in general, allow explicit correlation between volume fraction and stiffness. However, this relation can be inferred via a curve fit of the effective modulus. This resulted in the variation of Young's modulus and fitted polynomial coefficients displayed in Fig. 2. Poisson's ratio was assumed to be constant ($v = 0.25$) in this analysis. The small magnitude of such variation is neglected for simplicity.

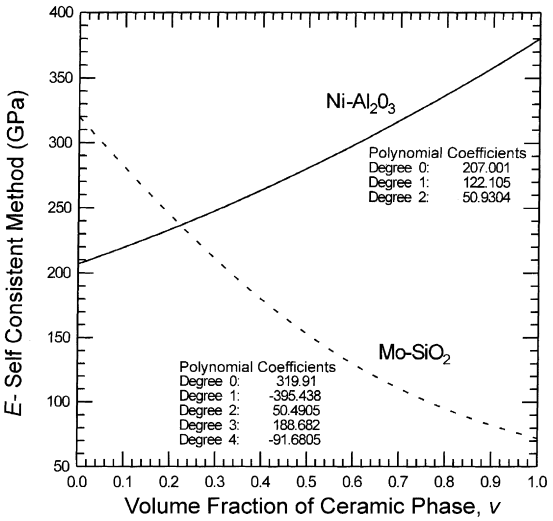

Fig. 2. Variation of effective Young's modulus, E, with composition for Mo–SiO_2 and Ni–Al_2O_3 composites according to the self-consistent method (SCM).

4. Results and discussion

4.1. Comparison with analytical solutions

As mentioned in Section 1, elasticity problems with varying modulus are much more difficult to solve than those with constant E, and therefore only the simplest one-dimensional cases can be considered. For the problems that can be solved analytically, restrictions must usually be placed on the allowable form of modulus variation. Specifically, a linear variation of modulus will be

[2] For problems with extreme modulus mismatch, the SCM cannot describe composites with the full range of composition (Christensen, 1990); however, this does not limit its application for the purpose of this study. Consideration was given to other micromechanical methods and differences in the results were negligible.

considered, varying from E_{metal} to E_{ceramic}. Similarly, unless specified otherwise the CTE was varied linearly from α_{metal} to α_{ceramic}. This does not necessarily represent the solution to problems for any specific material gradient, linear or otherwise. These analyses are formulated in terms of E and α; in contrast, problems formulated in terms of the material gradient parameters, v_i, will be addressed in Section 4.2.

Several simple FGM structures were analyzed and their thermal stress state computed, some self-constrained, other constrained by bonding to a massive material with $\alpha = 0$. This exact solution is then compared to that of homogeneous "average-modulus" problem with $E_{\text{ave}} = (E_{\text{metal}} + E_{\text{ceramic}})/2$ and to the approximate solution (Eq. (12)).

For the film on a rigid substrate with $\alpha = 0$ (Fig. 3), the solution displacement, $\boldsymbol{u}$, is independent of the modulus variation, therefore the approximate method yields the exact solution. These solutions of do not require any specific form of $E(z)$ (although a linear function was used for the data in Fig. 3). The general form for the residual stress after a temperature change, ΔT, is

$$\sigma_{xx} = \sigma_{yy} = -\frac{E(z)\alpha(z)\Delta T}{(1-\nu)}, \tag{14a}$$

$$\sigma_{zz} = 0. \tag{14b}$$

Also consider the problem of an axially graded peg in a rigid hole. If only radial contraction is restricted and the ends are free, then Eq. (14) represents the solution as well. If axial motions are also fixed, then for a peg with a small diameter the solution displacement will tend towards $\boldsymbol{u} = \boldsymbol{0}$. Normal stresses will coincided with Eq. (14a) after scaling by a factor of $(1-2\nu)/(1-\nu)$.

Lutz and Zimmerman (1996) solved the problem of an FGM sphere with free boundaries and with modulus and CTE being linear functions of radial position. The analytical solution was applied for both material sets for both the full $E(r)$ and $\alpha(r)$ problem and for homogeneous E_0. The homogeneous solution was used to compute the "average modulus" and approximate (Eq. (12)) stress states. Fig. 4 displays their exact solution for

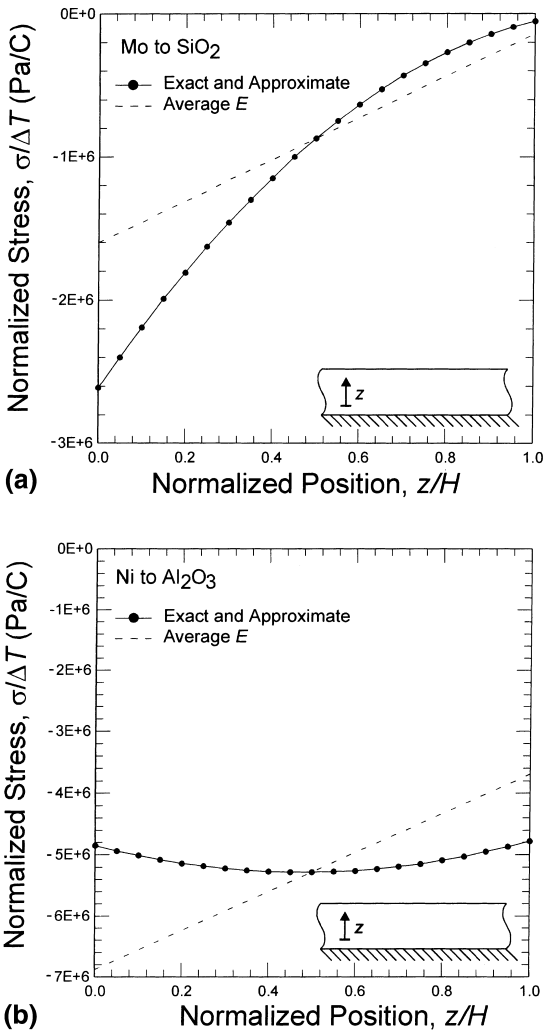

Fig. 3. FGM film on a rigid substrate undergoing temperature change ΔT. For this geometry the approximate solution coincides with the analytical.

tangential stress, $\sigma_{\theta\theta}$, with the approximate method and with the homogeneous E_{ave} solution. Eq. (12). was found to well incorporate the modulus effect, mapping the linear variation of stress (as seen in the "average E" dashed line) into a nonlinear distribution more like the full solution. Although at $r = 0$ the difference between the exact and the approximate is large (40% in the Mo–SiO_2 case), at the location of greatest importance for particle cracking, $r = R_0$, the difference is only 10%. Ignoring the effect of varying modulus, as in

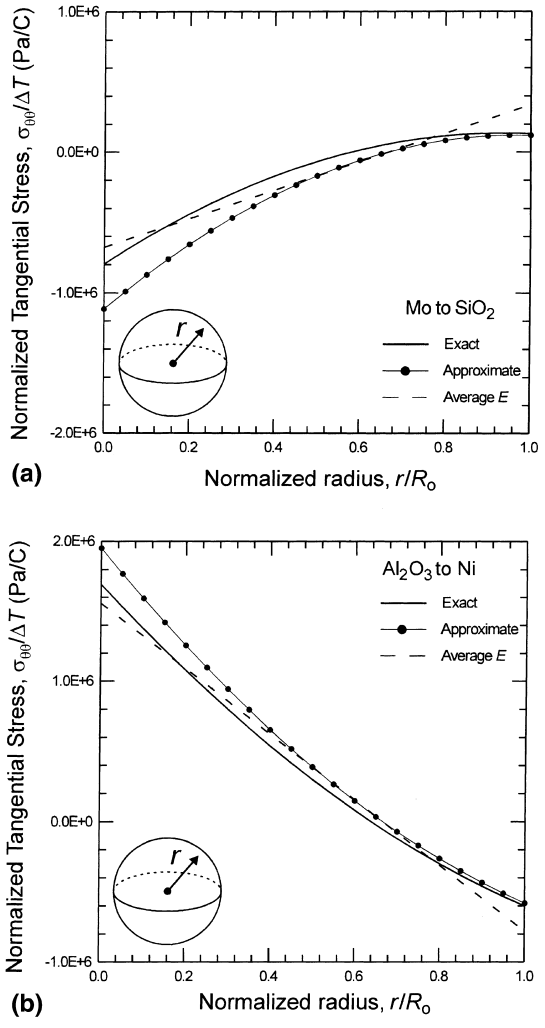

Fig. 4. FGM sphere undergoing free expansion. Note the order of the materials for this case: (a) Mo to SiO_2 and (b) Al_2O_3 to Ni (from stiffer to more compliant) is dictated by the restrictions on the analytical solution (Lutz and Zimmerman, 1996).

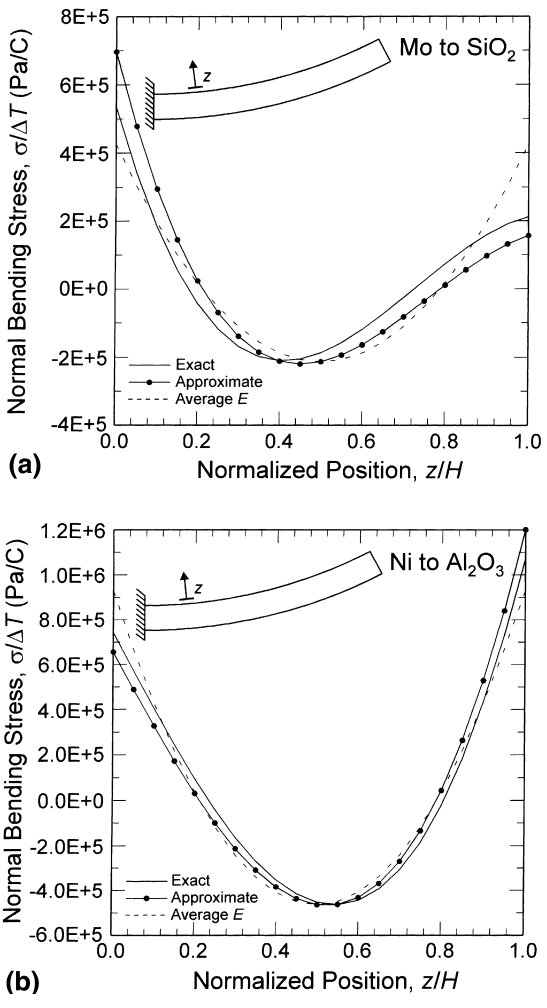

Fig. 5. FGM beam allowed to bend due to nonlinear CTE variation through its thickness.

the E_{ave} case, leads to $\sim$10 times the error at the surface.

For the free beam with a linear E gradient (similar to Giannakopoulos et al., 1995), a linear $\alpha(z)\Delta T$ will cause the beam to bend, but will result in a stress-free final configuration. Therefore, the beam problem was chosen with $\alpha(z) = \alpha_{metal} + (\alpha_{ceramic} - \alpha_{metal})(z/H)^2$, with the resulting stresses displayed in Fig. 5. For both the materials sets, Eq. (12) skews the symmetric stress variation (as in the "average E" dashed line) such that stresses are higher in the region with the stiffer material.

For a film sandwiched between two rigid platens ($\alpha = 0$) (Fig. 6) the approximate solution does not yield accurate results. The cause of this is the redistribution of strain (compared to the homogeneous E case) from stiffer regions to more compliant regions. A simple case to consider would be that of two springs in series held at constant nonzero displacement. As the stiffness of one spring increased, its displacement would decrease, requiring an increase in displacement in the other spring.

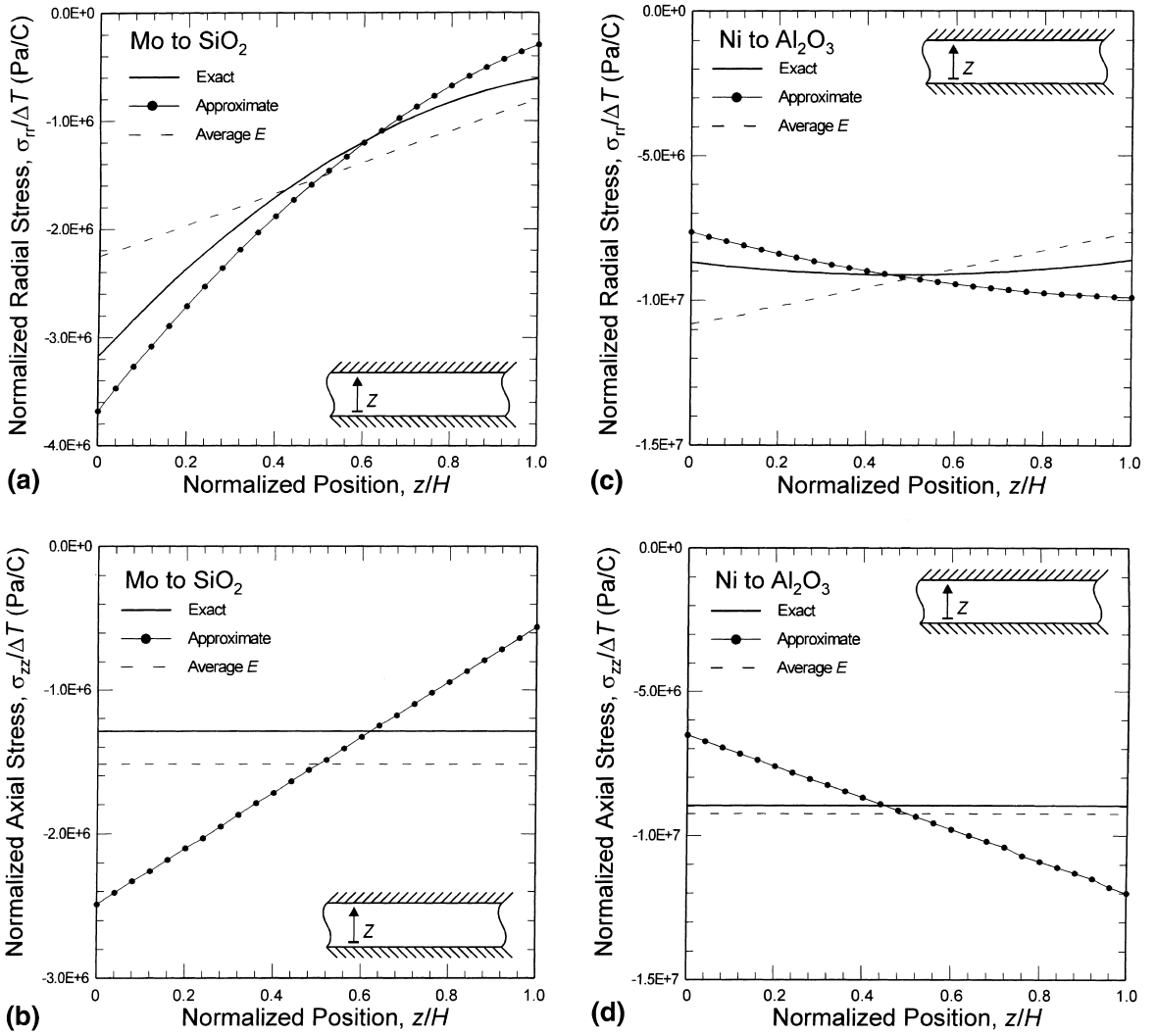

Fig. 6. FGM film sandwiched between rigid platens undergoing temperature change ΔT. The redistribution of strain as a function of local modulus leads to a solution that is not amenable to this approximate method.

Highly constrained problems represent the upper bound for thermal stresses, which, in the absence of this internal redistribution will tend to the exact $\boldsymbol{u} = \mathbf{0}$ solution discussed previously. For bodies with finite thickness, however, displacements will be affected by $E(z)$ such that Eq. (12) is inaccurate. In contrast, for bodies that are free to expand at their boundaries (such as deposited films or ceramics manufactured by free sintering), it is clear that Eq. (12) can provide accurate (or exact) results.

4.2. The axially graded cylinder

The joining of a metal/glass seal is one potential application for FGMs (Ishibashi et al., 1997). FGM parts are manufactured using a free-sintering method where the residual stresses arise from the cool-down from the sintering temperature. The corresponding mechanics problem is that of a right cylinder with free boundaries and the gradient along the z-direction. This is a two-dimensional problem, allowing contraction in both the radial

and axial directions. Lacking an analytical solution to this problem, FEA is used to compare the approximate method to complete FGM solutions.

4.2.1. Stress functions for an FGM cylinder

Using methods described in Section 3 (with constant modulus), the stress functions were calculated. The stress functions S^2_{zz}, $S^2_{\theta\theta}$, S^3_{zz} and $S^3_{\theta\theta}$, i.e., those corresponding to the residual cool-down stress for quadratic and cubic gradients, are shown in Figs. 7(a) and (b), at the centerline ($r = 0$) and surface ($r = R_0$). Fig. 8 displays the radial variations midway along the cylinder, $z = L/2$. Note that at the centerline, the circumferential and radial stress components are equal ($S^i_{rr} = S^i_{\theta\theta}$ at $r = 0$), as dictated by equilibrium considerations, and at the free lateral surface, $S^i_{rr} = 0$.

4.2.2. Gradients with the same compositional curvature

Since the constant and linear aspects of a thermal gradient do not contribute to the residual stress state, the deviation from linearity can be considered to be the "driving force" for residual thermal stresses. As discussed earlier, for problems with constant modulus, the residual stresses scale exactly linearly with the magnitudes of these deviations (the coefficients v_i, $i \geqslant 2$). Therefore, for such a material, the three gradients in the insert of Fig. 9, each with $v_2 = -0.001/\text{mm}^2$, will result in an identical residual stress state. However, for a Ni–Al_2O_3 FGM, with the moduli of the components differing by 83%, the residual stresses will increase with increasing average gradient (and, in this case, average Al_2O_3 volume fraction). This is shown by the symbols in Fig. 9, which represent the centerline stresses per degree of cool-down, calculated via FEA. This demonstrates that the effect of the gradient in elastic modulus on the residual stress state is substantial and that the deviation from linearity does not entirely predict the result (~20% difference between the cases). However, using the homogeneous stress function S^2_{zz} and by employing the approximation in Eq. (12) (solid lines), it is apparent that the error incurred is slight (less than 1% error between Eq. (12) and the full FEA results). Restated, for problems with variations in both thermal and elastic constants, the effect of modulus mismatch can be captured quite accurately by Eq. (12).

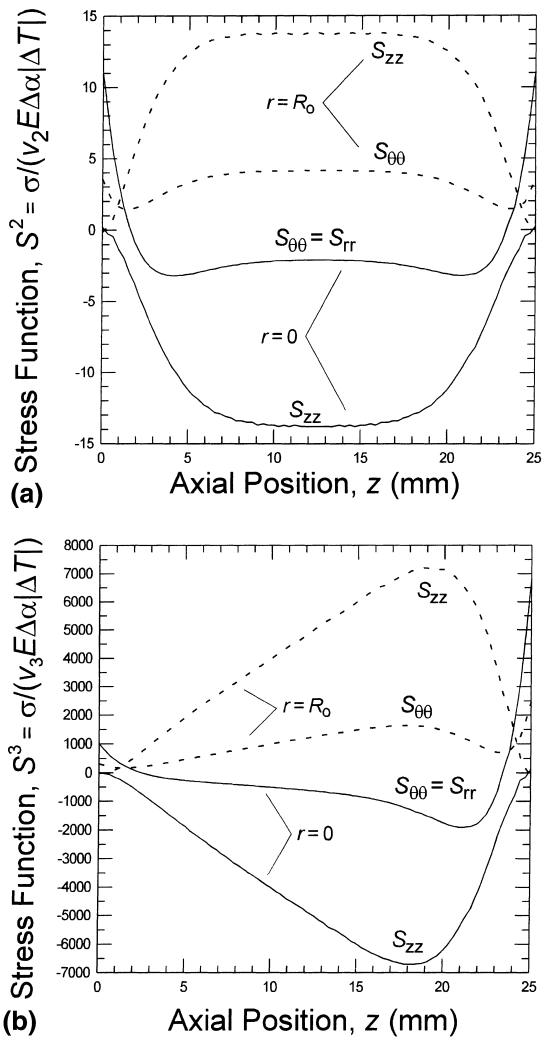

Fig. 7. (a) Quadratic stress function, S^2_{ij}, along the centerline ($r = 0$) and surface ($r = R_0$) for stress components $ij = \theta\theta$, zz. (b) Cubic stress function, S^3_{ij}, along the centerline ($r = 0$) and surface ($r = R_0$) for stress components $ij = \theta\theta$, zz.

4.2.3. Gradients with the differing compositional curvature

In addition to comparing gradients with the same curvature, the series in Fig. 10 can be considered. For each gradient, the composition changes smoothly from 10% to 90% ceramic with the

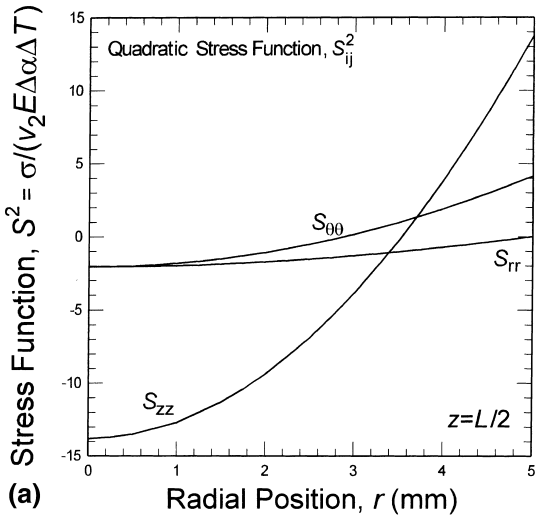

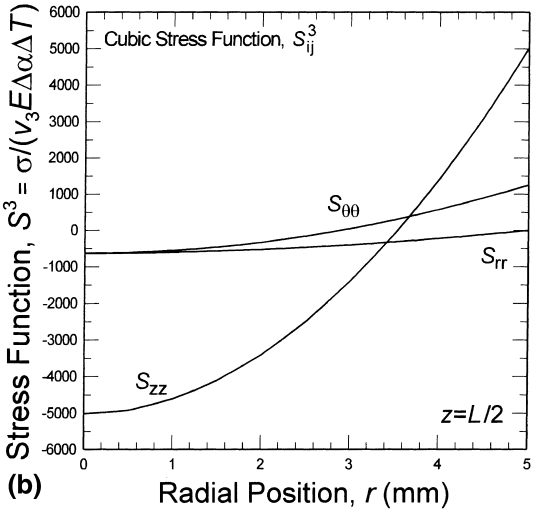

Fig. 8. (a) Radial variation of S_{ij}^2 and (b) of S_{ij}^3 at $z = L/2$.

balance being the metal phase. Each gradient is a quadratic function of axial position with $v_2 = 0.002, 0.001, 0.0, -0.001,$ and -0.002 mm^{-2}. Both of the material systems were considered for each of the gradients and the axial residual stresses per degree of cool-down $\sigma_{zz}/|\Delta T|$ are displayed as symbols in Figs. 11(a) and (b) and Figs. 12(a) and (b). The strong influence of gradient curvature on residual stress can be seen in both figures.

Results are broadly similar between the two material systems, with a few noticeable differences.

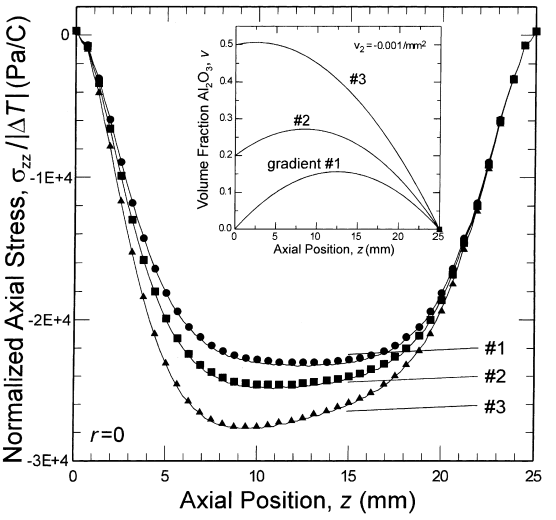

Fig. 9. The axial residual stress component, σ_{zz}, resulting from the three quadratic gradients (insert), each with the same curvature ($v_2 = -0.001$ mm^{-2}). The approximation of Eq. (12) for each of the gradients (solid lines) closely matches the finite element results (closed symbols).

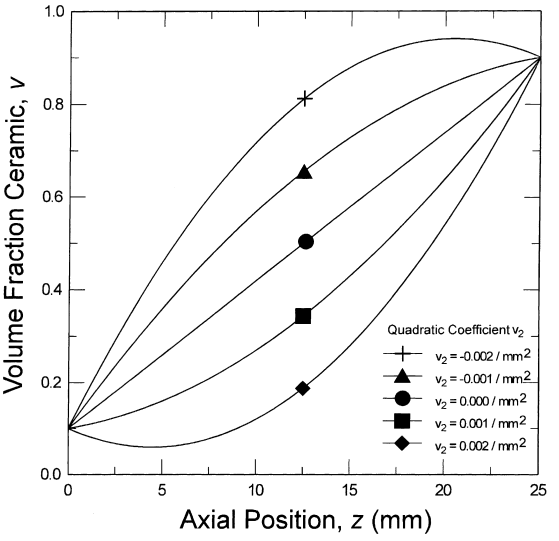

Fig. 10. A series of gradients with varying curvatures. The symbol on each curve indicates the value of the curvature such that the symbols +, ▲, ●, ■, ◆ correspond respectively to $v_2 = -0.002, -0.001, 0.0, 0.001,$ and 0.002 mm^{-2}.

For gradients with a positive curvature ($v_2 > 0$), the residual stress is compressive on the surface ($r = R_0$). For brittle materials where the overall

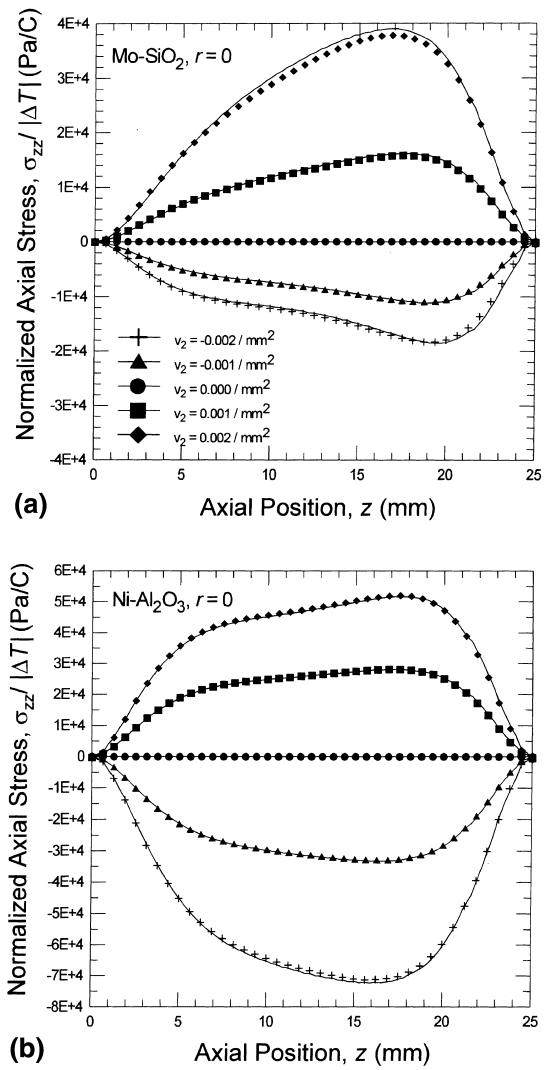

Fig. 11. Residual stresses along the centerline resulting from the gradients in Fig. 10 for the (a) Mo–SiO_2 and the (b) Ni–Al_2O_3 system. FGM calculations (symbols) are accurately approximated by Eq. (12) (solid lines).

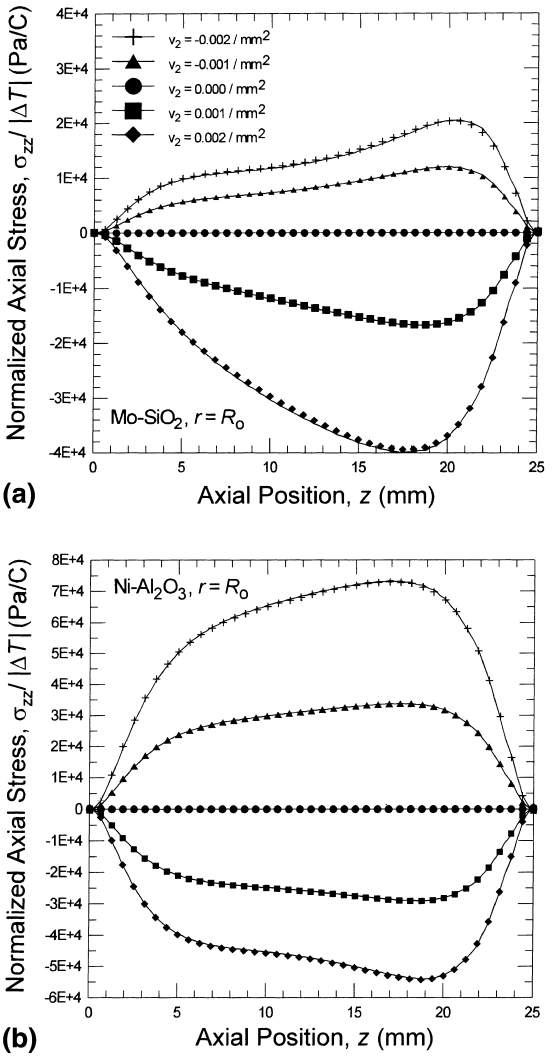

Fig. 12. Residual stresses along the surface resulting from the gradients in Fig. 10 for the (a) Mo–SiO_2 and the (b) Ni–Al_2O_3 system. FGM calculations (symbols) are accurately approximated by Eq. (12) (solid lines).

strength is greatly controlled by surface flaws, this can be regarded as a more favorable condition than stress-free.

As can be seen in Fig. 11, the relation between v_2 and σ postulated in Eq. (12) holds well even including the effects of $E(z)$. For some composites, Eq. (2) may not hold and a nonlinear composition-CTE relation should be used. In such a case the achievement of a favorable compressive stress-state upon cool-down would be dependent not on $v_2 = (1/2)\mathrm{d}^2v/\mathrm{d}z^2 > 0$ but on

$$\frac{\mathrm{d}^2\alpha}{\mathrm{d}z^2} = \left(\frac{\partial v}{\partial z}\right)^2 \frac{\partial^2\alpha}{\partial v^2} + \frac{\partial^2 v}{\partial z^2}\frac{\partial \alpha}{\partial v} < 0. \tag{15}$$

Both $\mathrm{d}\alpha/\mathrm{d}v$ and $\mathrm{d}^2\alpha/\mathrm{d}v^2$ would be determined by the specific micromechanical model used, but for a typical metal/ceramic FGM the former would be expected to be negative (i.e., $\alpha_{\mathrm{ceramic}} < \alpha_{\mathrm{metal}}$).

Therefore, for a quadric material gradient a positive value of $v_2\Delta\alpha\Delta T$ would still be desirable.

The solid lines in Figs. 11(a) and (b) and Figs. 12(a) and (b) represent the application of Eq. (12). The stress states of the SiO_2–Mo system are more asymmetric in the z-direction due to the greater mismatch in Young's modulus. It is apparent that this is a good approximation for either material system, although the error incurred is greater for the larger curvatures. This follows because the coupling effect of elastic gradient change and residual stress, as described in Section 2.2.

4.2.4. Sigmoidal gradients

Previous discussion has been limited to polynomial gradients. For certain problems a polynomial description of the gradient is advantageous and allows the superposition of $\alpha\Delta T$ fields. However, Eq. (12) is in no way restricted to such gradients. Sigmoidal gradient shapes are important since they simulate grading resulting from the interdiffusion of two materials.

Hyperbolic tangent gradients are shown in the insert of Fig. 13 and the surface residual stresses calculated via FEA for the Ni–Al_2O_3 system are displayed as the symbols in Fig. 13. The approximation (Eq. (12)) results are shown as solid lines.

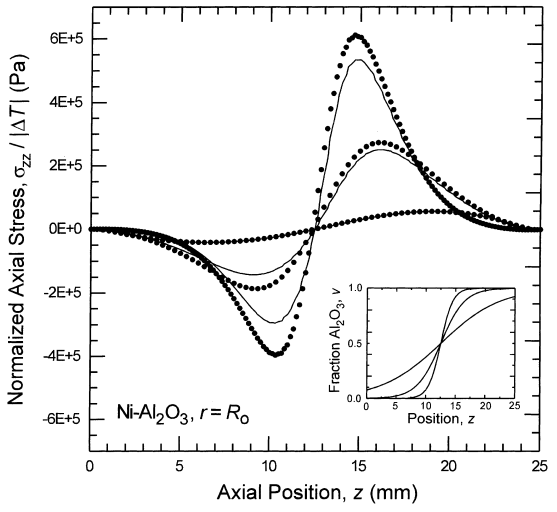

Fig. 13. The surface residual zz-stresses resulting from the series of sigmodial gradients (insert). The finite element results (symbols) are approximated by Eq. (12) (lines).

For the sigmoidal gradient, areas of positive gradient curvature correspond to a beneficial compressive stress at the surface. Likewise, areas of negative gradient curvature correspond to a tensile stress, in agreement with the results for the quadratic gradients (Fig. 12(b)).

As in the case of the pure quadratic, the approximation for the residual stresses works well; however, the error in the steepest of the sigmoidal gradients is indicative of the limitations of this procedure for problems with rapid changes in modulus. Still, for the sharpest gradient studied the error in the approximation of the maximum σ_{zz} was less than 15% even though the transition from 10% to 90% Al_2O_3 took place within a distance of $L/5$.

5. Summary

A method is presented for approximating the residual stress state in an FGM structure with free surfaces. For FGM films, the results of the approximation coincide with the exact solution. Numerical solutions for an FGM cylinder have shown this method to be accurate within 15% for all gradients studied. The method allows the application of a wide class of homogeneous-modulus residual stress analyses to FGMs. This allows, at lower cost than a full finite element analysis, the identification of favorable and unfavorable aspects of the gradient nonlinearity, for either avoiding stresses or building desirable surface compressive stresses.

Acknowledgements

This work was supported by the Director, Office of Energy Research, Office of Basic Energy Sciences, Materials Sciences Division of the US Department of Energy under Contract No. DE-AC03-76SF00098. Additional support was provided by the TOTO Corporation. The authors would like to thank Prof. Panos Papadopoulos for helpful discussions regarding Section 2.2.

References

Boley, B., Winer, J., 1985. Theory of Thermal Stresses. R.E. Krieger Pub. Co., Malabar, Fla.

Christensen, R.M., 1990. A critical evaluation for a class of micro-mechanics models. J. Mech. Phys. Solids 38, 379–404.

Delfosse, D., Kunzi, H.-U., Ilschner, B., 1992. Experimental determination of residual stresses with a one-dimensional gradient of composition. Acta Metall. Mater. 40, 2219–2224.

Giannakopoulos, A.E., Suresh, S., Finot, M., Olsson, M., 1995. Elastoplastic analysis of thermal cycling: layered materials with compositional gradients. Acta Metall. Mater. 43, 1335–1354.

Grujicic, M., Zhao, H., 1998. Optimization of 316 stainless steel/alumina functionally graded material for reduction of damage induced by thermal residual stresses. Mater. Sci. Eng. A A252, 117–132.

Hill, R., 1965. A self-consistent mechanics of composite materials. J. Mech. Phys. Solids 13, 213–222.

Hoger, A., 1986. On the determination of residual stress in an elastic body. J. Elasticity 16, 303–324.

Ishibashi, H., Saiz, E., Tomsia, A.P., 1997. Mo/SiO_2 FGMs fabricated by slip casting. Am. Ceram. Soc. Bull. 76, 231.

Lutz, M.P., Zimmerman, R.W., 1996. Thermal stresses and effective thermal expansion coefficient of a functionally gradient sphere. J. Thermal Stress 19, 39–54.

Markworth, A.J., Saunders, J.H., 1995. A model of structure optimization for a functionally graded material. Mater. Lett. 22, 103–107.

Nikishin, V.S., 1966. Thermal Stresses in a Composite Cylinder with an Arbitrary Temperature Distribution along its Length. Plenum Press, Data Division, New York.

Obata, Y., Noda, N., 1994. Steady thermal stresses in a hollow circular cylinder and a hollow sphere of a functionally gradient material. J. Thermal Stresses 17, 471–487.

Rabin, B.H., Williamson, R.L., Bruck, H.A., Wang, X.-L. et al., 1998. Residual strains in Al_2O_3 joint bonded with a composition interlayer: experimental measurements and FEM analysis. J. Amer. Cer. Soc. 81, 1541–1549.

Ravichandran, K.S., 1995. Thermal residual stresses in a functionally graded material system. Mater. Sci. Eng. A A201, 269–276.

Tanaka, K., Watanabe, H., Sugano, Y., 1996. A multicriterial material tailoring of a hollow cylinder in functionally gradient materials: scheme to global reduction of thermo-elastic stresses. Comput. Meth. Appl. Mech. Eng. 135, 369–380.

Tanigawa, Y., Akai, T., Kawamura, R., Oka, N., 1996. Transient heat conduction and thermal stress problems of a nonhomogeneous plate with temperature-dependent material properties. J. Thermal Stresses 19, 77–102.

Touloukian, Y.S. (Ed.), 1975. Thermal expansion-metallic elements and alloys. Thermophysical Properties of Matter. IFI/Plenum, New York.

Touloukian, Y.S. (Ed.), 1977. Thermal expansion-nonmetallic solids. Thermophysical Properties of Matter. IFI/Plenum, New York.

Zienkiewicz, O.C., Taylor, R.L., 1987. The Finite Element Method. McGraw-Hill, New York.

Zuiker, J.R., 1995. Functionally graded materials: choice of micromechanical model and limitations in property variation. Compos. Eng. 5, 807–819.